Measurement of Cross Sections for $D^0\bar{D}^0$ and D^+D^- Production in e^+e^- Annihilation at $\sqrt{s} = 3.773$ GeV

M. Ablikim[1], J. Z. Bai[1], Y. Ban[10], J. G. Bian[1], X. Cai[1], J. F. Chang[1], H. F. Chen[15], H. S. Chen[1], H. X. Chen[1], J. C. Chen[1], Jin Chen[1], Jun Chen[6], M. L. Chen[1], Y. B. Chen[1], S. P. Chi[2], Y. P. Chu[1], X. Z. Cui[1], H. L. Dai[1], Y. S. Dai[17], Z. Y. Deng[1], L. Y. Dong[1], S. X. Du[1], Z. Z. Du[1], J. Fang[1], S. S. Fang[2], C. D. Fu[1], H. Y. Fu[1], C. S. Gao[1], Y. N. Gao[14], M. Y. Gong[1], W. X. Gong[1], S. D. Gu[1], Y. N. Guo[1], Y. Q. Guo[1], K. L. He[1], M. He[11], X. He[1], Y. K. Heng[1], H. M. Hu[1], T. Hu[1], L. Huang[6], X. P. Huang[1], X. B. Ji[1], Q. Y. Jia[10], C. H. Jiang[1], X. S. Jiang[1], D. P. Jin[1], S. Jin[1], Y. Jin[1], Y. F. Lai[1], F. Li[1], G. Li[1], H. H. Li[1], J. Li[1], J. C. Li[1], Q. J. Li[1], R. B. Li[1], R. Y. Li[1], S. M. Li[1], W. G. Li[1], X. L. Li[7], X. Q. Li[9], X. S. Li[14], Y. F. Liang[13], H. B. Liao[5], C. X. Liu[1], F. Liu[5], Fang Liu[15], H. M. Liu[1], J. B. Liu[1], J. P. Liu[16], R. G. Liu[1], Z. A. Liu[1], Z. X. Liu[1], F. Lu[1], G. R. Lu[4], J. G. Lu[1], C. L. Luo[8], X. L. Luo[1], F. C. Ma[7], J. M. Ma[1], L. L. Ma[11], Q. M. Ma[1], X. Y. Ma[1], Z. P. Mao[1], X. H. Mo[1], J. Nie[1], Z. D. Nie[1], H. P. Peng[15], N. D. Qi[1], C. D. Qian[12], H. Qin[8], J. F. Qiu[1], Z. Y. Ren[1], G. Rong[1], L. Y. Shan[1], L. Shang[1], D. L. Shen[1], X. Y. Shen[1], H. Y. Sheng[1], F. Shi[1], X. Shi[10], H. S. Sun[1], S. S. Sun[15], Y. Z. Sun[1], Z. J. Sun[1], X. Tang[1], N. Tao[15], Y. R. Tian[14], G. L. Tong[1], D. Y. Wang[1], J. Z. Wang[1], K. Wang[15], L. Wang[1], L. S. Wang[1], M. Wang[1], P. Wang[1], P. L. Wang[1], S. Z. Wang[1], W. F. Wang[1], Y. F. Wang[1], Zhe Wang[1], Z. Wang[1],Zheng Wang[1], Z. Y. Wang[1], C. L. Wei[1], D. H. Wei[3], N. Wu[1], Y. M. Wu[1], X. M. Xia[1], X. X. Xie[1], B. Xin[7], G. F. Xu[1], H. Xu[1], Y. Xu[1], S. T. Xue[1], M. L. Yan[15], F. Yang[9], H. X. Yang[1], J. Yang[15], S. D. Yang[1], Y. X. Yang[3], M. Ye[1], M. H. Ye[2], Y. X. Ye[15], L. H. Yi[6], Z. Y. Yi[1], C. S. Yu[1], G. W. Yu[1], C. Z. Yuan[1], J. M. Yuan[1], Y. Yuan[1], Q. Yue[1], S. L. Zang[1],Yu. Zeng[1], Y. Zeng[6], B. X. Zhang[1], B. Y. Zhang[1], C. C. Zhang[1], D. H. Zhang[1], H. Y. Zhang[1], J. Zhang[1], J. Y. Zhang[1], J. W. Zhang[1], L. S. Zhang[1], Q. J. Zhang[1], S. Q. Zhang[1], X. M. Zhang[1], X. Y. Zhang[11], Y. J. Zhang[10], Y. Y. Zhang[1], Yiyun Zhang[13], Z. P. Zhang[15], Z. Q. Zhang[4], D. X. Zhao[1], J. B. Zhao[1], J. W. Zhao[1], M. G. Zhao[9], P. P. Zhao[1], W. R. Zhao[1], X. J. Zhao[1], Y. B. Zhao[1], H. Q. Zheng[10], J. P. Zheng[1], L. S. Zheng[1], Z. P. Zheng[1], X. C. Zhong[1], B. Q. Zhou[1], G. M. Zhou[1], L. Zhou[1], N. F. Zhou[1], K. J. Zhu[1], Q. M. Zhu[1], Y. C. Zhu[1], Y. S. Zhu[1], Yingchun Zhu[1], Z. A. Zhu[1], B. A. Zhuang[1], B. S. Zou[1],

(BES Collaboration)

[1] *Institute of High Energy Physics, Beijing 100039, People's Republic of China*
[2] *China Center for Advanced Science and Technology, Beijing 100080, People's Republic of China*
[3] *Guangxi Normal University, Guilin 541004, People's Republic of China*
[4] *Henan Normal University, Xinxiang 453002, People's Republic of China*
[5] *Huazhong Normal University, Wuhan 430079, People's Republic of China*
[6] *Hunan University, Changsha 410082, People's Republic of China*
[7] *Liaoning University, Shenyang 110036, People's Republic of China*
[8] *Nanjing Normal University, Nanjing 210097, People's Republic of China*
[9] *Nankai University, Tianjin 300071, People's Republic of China*
[10] *Peking University, Beijing 100871, People's Republic of China*
[11] *Shandong University, Jinan 250100, People's Republic of China*
[12] *Shanghai Jiaotong University, Shanghai 200030, People's Republic of China*
[13] *Sichuan University, Chengdu 610064, People's Republic of China*
[14] *Tsinghua University, Beijing 100084, People's Republic of China*
[15] *University of Science and Technology of China, Hefei 230026, People's Republic of China*
[16] *Wuhan University, Wuhan 430072, People's Republic of China*
[17] *Zhejiang University, Hangzhou 310028, People's Republic of China*

The cross sections for $D^0\bar{D}^0$ and D^+D^- production at 3.773 GeV have been measured with BES-II detector at BEPC. These measurements are made by analyzing a data sample of about 17.3 pb^{-1} collected at the center-of-mass energy of 3.773 GeV. Observed cross sections for the charm pair production are radiatively corrected to obtain the tree level cross section for $D\bar{D}$ production. A measurement of the total tree level hadronic cross section is obtained from the tree level $D\bar{D}$ cross section and an extrapolation of the R_{uds} below the open charm threshold.

PACS numbers:

I. INTRODUCTION

Around the center-of-mass energy of 3.770 GeV, the open charm pairs, $D^0\bar{D}^0$ and D^+D^-, are mainly produced in $\psi(3770)$ decays. So the measurement of the cross sections for $D^0\bar{D}^0$ and D^+D^- production at an en-

ergy point around 3.770 GeV is very important in the understanding of $\psi(3770)$ decays. A coupled-channel model [1] predicts that the cross section for $\psi(3770)$ production is about 3 nb and that the $\psi(3770)$ decay exclusively into $D^0\bar{D}^0$ and D^+D^-. Experimental results on the measurement of the $D^0\bar{D}^0$, D^+D^- and $D\bar{D}$ cross sections can be used to test the theoretical prediction. Also the measured values of the cross sections can be used to determine the branching fraction for $\psi(3770) \to \text{non}D\bar{D}$ using the measured cross section for $\psi(3770) \to$ hadrons at the same energy point. The determination of the partial width of $\psi(3770) \to \text{non}D\bar{D}$ has great interest since it would be helpful for investigating the mixing between S and D waves in its wave function [2], and in turn to help in developing the Potential Model [1].

In addition, by adding the tree level open charm cross section to an extrapolation of the tree level hadronic cross section for the light hadron production in the region below the open charm threshold, the total tree level hadronic cross section can be obtained [3][4]. The tree level cross section for inclusive hadronic event production in the e^+e^- annihilation at all energies is needed to calculate the effects of vacuum polarization on the parameters of the Standard Model. The largest uncertainty in this calculation arises from the uncertainties in the measured inclusive hadronic cross sections in the open charm threshold region. Traditionally, the tree level hadronic cross sections are measured by counting inclusive hadronic events. Using the measured cross sections for the $D\bar{D}$ production in the charm threshold region, we can also measure the tree level inclusive hadronic cross sections.

II. THE BES-II DETECTOR

BES-II is a conventional cylindrical magnetic detector that is described in detail in Ref. [5]. A 12-layer vertex chamber (VC) surrounding the beryllium beam pipe provides input to the event trigger, as well as coordinate information. A forty-layer main drift chamber (MDC) located just outside the VC yields precise measurements of charged particle trajectories with a solid angle coverage of 85% of 4π; it also provides ionization energy loss (dE/dx) measurements which are used for particle identification. Momentum resolution of $1.7\%\sqrt{1+p^2}$ (p in GeV/c) and dE/dx resolution of 8.5% for Bhabha scattering electrons are obtained for the data taken at $\sqrt{s}$ = 3.773 GeV. An array of 48 scintillation counters surrounding the MDC measures the time of flight (TOF) of charged particles with a resolution of about 180 ps for electrons. Outside the TOF, a 12 radiation length, lead-gas barrel shower counter (BSC), operating in limited streamer mode, measures the energies of electrons and photons over 80% of the total solid angle with an energy resolution of $\sigma_E/E = 0.22/\sqrt{E}$ (E in GeV) and spatial resolutions of σ_ϕ = 7.9 mrad and σ_Z = 2.3 cm for electrons. A solenoidal magnet outside the BSC provides a 0.4 T magnetic field in the central tracking region of the detector. Three double-layer muon counters instrument the magnet flux return and serve to identify muons with momentum greater than 500 MeV/c. They cover 68% of the total solid angle.

III. DATA SAMPLE AND METHOD TO DETERMINE $\sigma_{D\bar{D}}$

The data used for this analysis were collected at the center-of-mass energy of 3.773 GeV with the Beijing Spectrometer [5] at Beijing Electron Positron Collider. The total integrated luminosity of the data set is 17.3 pb^{-1}, which is obtained based on analysis of large angle Bhabha scattering from the same data set.

The measurements of the cross sections for the $D^0\bar{D}^0$ and D^+D^- production are made based on the analysis of singly tagged D^0 and D^+ events. At the center-of-mass energy $\sqrt{s}$ = 3.773 GeV, the D^0 (through this paper, charge conjugation is implied) and D^+ are produced in pair via the process of

$$e^+e^- \to D^0\bar{D}^0, D^+D^-. \tag{1}$$

The total observed number $N_{D^0_{\rm tag}}$ ($N_{D^+_{\rm tag}}$) of D^0 (D^+) meson and the observed cross section $\sigma^{\rm obs}_{D^0\bar{D}^0}$ ($\sigma^{\rm obs}_{D^+D^-}$) are related as

$$\sigma^{\rm obs}_{D^0\bar{D}^0} = \frac{N_{D^0_{\rm tag}}}{2\times L\times B\times\epsilon}, \tag{2}$$

and

$$\sigma^{\rm obs}_{D^+D^-} = \frac{N_{D^+_{\rm tag}}}{2\times L\times B\times\epsilon}, \tag{3}$$

where L is the integrated luminosity of the data set used in the analysis, B is the branching fraction for decay mode in question, and ϵ is the efficiency determined from Monte Carlo for reconstruction of this decay mode.

In the measurements of the cross sections, the singly tagged neutral and charged D mesons are observed in the invariant mass spectra of the daughter particles from the D decay.

IV. DATA ANALYSIS

A. Event selection

The neutral and charged D mesons are reconstructed in the final states of $K^-\pi^+$, $K^-\pi^+\pi^+\pi^-$ and $K^-\pi^+\pi^+$. Events which contain at least two reconstructed charged-tracks with good helix fits are selected. In order to ensure well-measured 3-momentum vectors and reliable charged-particle identification, the charged tracks used in the single tag analysis are required to be within $|cos\theta|$ <0.85, where θ is the angle with respect to beam direction. All

TABLE I: Singly tagged D^0 and D^+ samples. Where the $M_{\rm fit}$ is the fitted mass of singly tagged D meson, the $N^{\rm obs}_{D_{\rm tag}}$ is the observed number of singly tagged D meson and the $N_{D_{\rm tag}}$ is the "true" number of the singly tagged D meson after correcting the contamination from other decay modes.

Tag Mode	$M_{\rm fit}$ [MeV/c^2]	$N^{\rm obs}_{D_{\rm tag}}$	$N_{D_{\rm tag}}$
$K^-\pi^+$	1865.5 ± 0.1	1642.8 ± 49.9	1627.4 ± 49.9
$K^-\pi^+\pi^+\pi^-$	1865.4 ± 0.1	1327.2 ± 48.6	1299.1 ± 48.6
$K^-\pi^+\pi^+$	1870.2 ± 0.1	2029.3 ± 57.4	2010.8 ± 57.4

tracks must originate from the interaction region, which require that the closest approach of the charged track in xy plane is less than 2.0 cm and the z position of the charged track is less than 20.0 cm. Pions and kaons are identified by means of TOF and dE/dx measurements. The pion identification requires a consistency with the pion hypothesis at a confidence level greater than 0.1%. In order to reduce misidentification, the kaon candidate is required to have a larger confidence level for a kaon hypothesis than that for a pion hypothesis.

B. Analysis of inclusive D meson events

Taking advantage of the $D\bar{D}$ pair production, we use a kinematic fit to candidate D^0 or D^+ decays to improve the ratio of signal to noise and mass resolution in the invariant mass spectrum. The energy-constraint is imposed on the measured momenta of the D daughter particles via the kinematic fit to improve the measured charged track three-momenta. Events with a kinematic fit probability greater than 1% are accepted. If more than one combination satisfies the fit probability greater than 1%, the combination with the largest fit probability is retained.

The resulting distributions of the fitted masses of $Km\pi$ (m = 1, or 2, or 3) combinations, which are calculated using the fitted momentum vectors from the kinematic fit, are shown in figure 1. The signals for D^0 and D^+ production are clearly observed in the fitted mass spectra. A maximum likelihood fit is performed to the mass spectrum, a Gaussian is used to model the signal shape and a special function [6] is used to describe the background shape. The D^0 and D^+ yields obtained from this fit is given in table I.

The same $Km\pi$ combinations from other decay modes can also pass the above selection criteria and the distributions of the fitted masses of the combinations are with a small peak around the masses of D mesons. The rates of the contaminations are evaluated to be 0.0094, 0.0212 and 0.0091 for the $D^0 \to K^-\pi^+$, $D^0 \to K^-\pi^+\pi^+\pi^-$ and $D^+ \to K^-\pi^+\pi^+$, respectively. After correcting the observed numbers of the singly tagged D events for these combinations, the "true" numbers of the D signal events for the three singly tagged D modes are obtained to be

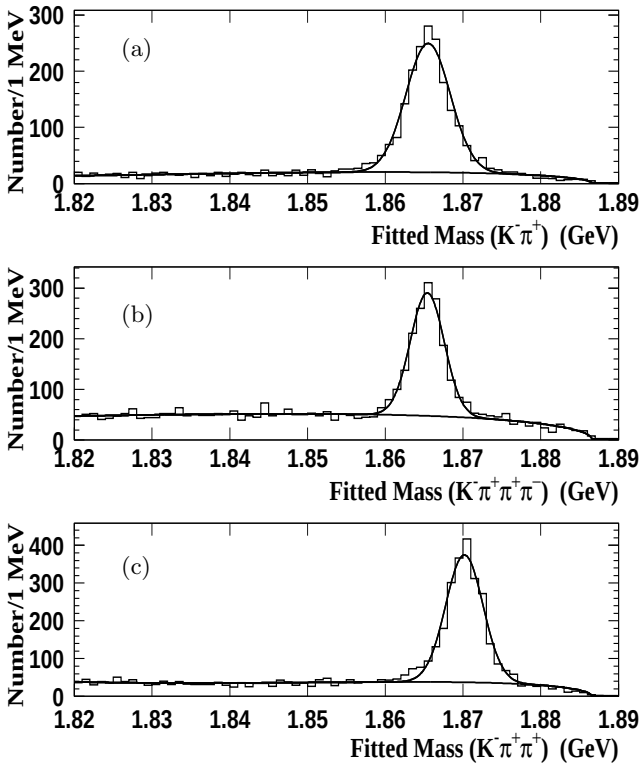

FIG. 1: Distribution of the fitted masses of the $Km\pi$ (m=1, or 2, or 3) combinations for three singly tagged modes, where figure (a) and figure (b) are for the decay modes of $D^0 \to K^-\pi^+$ and $D^0 \to K^-\pi^+\pi^+\pi^-$, respectively, and the figure (c) is for the decay mode of $D^+ \to K^-\pi^+\pi^+$.

1627 ± 50, 1299 ± 49 and 2011 ± 57. Table I summarizes the results of the inclusive D analysis.

V. OBSERVED CROSS SECTIONS FOR $D^0\bar{D}^0$ AND D^+D^- PRODUCTION

A. Monte Carlo Efficiency

To estimate the reconstructed efficiencies of $D^0 \to K^-\pi^+$, $D^0 \to K^-\pi^+\pi^+\pi^-$ and $D^+ \to K^-\pi^+\pi^+$, the Monte Carlo samples of $D\bar{D}$ production and decays are generated according to equation (1), where the ratio of the neutral over the total $D\bar{D}$ production cross section is set to be 0.58. Both D and $\bar{D}$ mesons decay to all possible modes according to the branching fractions quoted from PDG[7]. The generated events are simulated with a GEANT based Monte Carlo package. All decay processes which contribute to the decay modes in question are considered in estimating the efficiencies. Detailed Monte Carlo studies give the efficiencies to be (35.26 ± 0.19)%, (13.73 ± 0.09)% and (25.00 ± 0.13)% for the reconstruction of $D^0 \to K^-\pi^+$, $D^0 \to K^-\pi^+\pi^+\pi^-$

TABLE II: Summary of the observed cross section times branching fraction.

Mode	$\sigma_{D\bar{D}} \times B$ [nb]
$D^0 \to K^-\pi^+$	$0.133 \pm 0.004 \pm 0.008$
$D^0 \to K^-\pi^+\pi^+\pi^-$	$0.273 \pm 0.010 \pm 0.025$
$D^+ \to K^-\pi^+\pi^+$	$0.233 \pm 0.007 \pm 0.018$

TABLE III: A comparison of $\sigma_D \times B$ measured by this experiment, MARK-I and MARK-II experiments.

Mode	$\sigma_D \times B$ [nb] (This experiment) $E_{cm} = 3.773$ GeV	$\sigma_D \times B$ [nb] (MARK-II) $E_{cm} = 3.771$ GeV	$\sigma_D \times B$ [nb] (MARK-I) $E_{cm} = 3.774$ GeV
$K^-\pi^+$	0.27 ± 0.02	0.24 ± 0.02	0.25 ± 0.05
$K^-\pi^+\pi^+\pi^-$	0.55 ± 0.05	0.68 ± 0.11	0.36 ± 0.10
$K^-\pi^+\pi^+$	0.47 ± 0.04	0.38 ± 0.05	0.36 ± 0.06

and $D^+ \to K^-\pi^+\pi^+$ decay modes, respectively.

B. Observed Cross Sections

Inserting the number of the singly tagged D events and the efficiencies for each of the three decay modes, the $\sigma_{D\bar{D}} \times B$ of $D^0\bar{D}^0$ and D^+D^- are obtained and the results are shown in table II. The first error is statistical and second systematic which arise from the uncertainty in the measured luminosity ($\sim 3\%$), tracking ($\sim 2\%$ per track), particle identification ($\sim 0.5\%$/track), kinematic fit ($\sim 1\%$), fitting parameters ($\sim 3\%$) and Monte Carlo statistics ($\sim 0.6\%$). The total systematic uncertainty is obtained by adding all systematic uncertainties in quadrature. A comparison of our measured $\sigma_D \times B$ with that measured by MARK-II [8] and MARK-I [9] is given in Table III. The observed cross section for D^+D^- production is obtained by dividing the $\sigma_{D\bar{D}} \times B$ by branching fraction quoted from PDG[7], which gives,

$$\sigma^{\rm obs}_{D^+D^-} = (2.56 \pm 0.08 \pm 0.26) \ \ {\rm nb}. \qquad (4)$$

The observed cross sections for $D^0\bar{D}^0$ production are $\sigma^{\rm obs}_{D^0\bar{D}^0} = (3.50 \pm 0.11)$ nb and $\sigma^{\rm obs}_{D^0\bar{D}^0} = (3.66 \pm 0.13)$ nb, which are determined from the analysis of the singly tagged modes of $D^0 \to K^-\pi^+$ and $D^0 \to K^-\pi^+\pi^+\pi^-$ respectively; where the errors are statistical. Averaging the two observed cross sections for $D^0\bar{D}^0$ production gives the average of the observed cross section for $D^0\bar{D}^0$ production to be

$$\sigma^{\rm obs}_{D^0\bar{D}^0} = (3.58 \pm 0.09 \pm 0.31) \ \ {\rm nb}, \qquad (5)$$

where the first error is statistical and second systematic which is estimated based on the averaged three charged tracks in the two modes of the single tags. Adding the observed cross sections of the neutral and charged modes together gives the observed cross section for $D\bar{D}$ production to be

$$\sigma^{\rm obs}_{D\bar{D}} = (6.14 \pm 0.12 \pm 0.50) \ \ {\rm nb}, \qquad (6)$$

where the first error is statistical and the second systematic. In the estimation of the systematic error of the $\sigma^{\rm obs}_{D\bar{D}}$, sources of systematic uncertainty are segregated into components that are common or independent for D^0 and D^+ measurements. The common components are the uncertainty in the measured integrated luminosity, the uncertainty in tracking and the uncertainty in particle identification. Since the absolute branching fraction scale for $D^+ \to K^-\pi^+\pi^+$ and $D^0 \to K^-\pi^+\pi^+\pi^-$ depend on the branching fraction scale for $D^0 \to K^-\pi^+$, the total percentage uncertainty for the two channel branching fractions (6.6% and 4.1%) are split into a common component that matches the percentage uncertainty for the $D^0 \to K^-\pi^+$ branching fraction (2.3%) and independent components (6.2% and 3.4%). All other systematic uncertainties are treated as independent and added in quadrature. The common uncertainties are added linearly.

TABLE IV: Comparison of the observed cross section with that measured by MARK-III [10] experiment.

	$\sigma^{\rm obs}_{D\bar{D}}$ [nb] (This experiment) $E_{cm} = 3.773$ GeV	$\sigma^{\rm obs}_{D\bar{D}}$ [nb] (MARK-III) $E_{cm} = 3.768$ GeV
$\sigma_{D^0\bar{D}^0}$	$3.58 \pm 0.09 \pm 0.31$	$2.90 \pm 0.25 \pm 0.30$
$\sigma_{D^+D^-}$	$2.56 \pm 0.08 \pm 0.26$	$2.10 \pm 0.30 \pm 0.15$

As a comparison, Table IV lists the observed cross sections for $D^0\bar{D}^0$ and D^+D^- production at the c.m. energies of 3.773 GeV and 3.768 GeV, which were measured by this experiment and MARK-III [10].

VI. RADIATIVE CORRECTIONS

In any e^+e^- colliding beam experiment, the electron (positron) always radiates at the interaction point because of the potential of the positron (electron). Since this radiation (Bremsstrahlung) carries energy away, the actual center-of-mass energy for the e^+e^- annihilation is reduced by Bremsstrahlung to $\sqrt{s(1-x)}$, where $xE_{\rm beam}$ is the total energy of the emitted photons. The Bremsstrahlung is principally responsible for the distortions to the tree level resonance line shape, while the self energy of the electron and positron and the vertex corrections to the initial state affect the overall factors to change the scale of the cross section. All of these corrections are called Initial State Radiation (ISR) corrections.

The tree level cross section for $D\bar{D}$ production at the energy of 3.773 GeV can be obtained by correcting the observed cross section for the effects of the ISR and vacuum polarization.

The observed cross section, $\sigma^{\rm obs}$, at the nominal energy $\sqrt{s}$ can be written as a convolution of the Born cross section $\sigma^B(s(1-x))$ and a sampling function $f(x,s)$,

$$\sigma^{\rm obs}(s) = \int_0^1 dx \cdot f(x,s)\sigma^B(s(1-x))(1+\delta_{VP}(s(1-x))). \tag{7}$$

The vacuum polarization correction $(1+\delta_{VP})$ includes both leptonic and hadronic terms. It varies from charm threshold to 4.14 GeV by less than $\pm 2\%$ [3]. In this data analysis, we treat it as a constant of

$$(1+\delta_{VP}) = 1.047 \pm 0.024. \tag{8}$$

Since we are interested in the $\psi(3770)$ resonance in this analysis, we take the σ^B to be the bare Breit-Wigner cross section

$$\sigma^B(E) = \frac{12\pi\Gamma^0_{ee}\Gamma_{\rm tot}(E)}{(E^2-M^2)^2 + M^2\Gamma^2_{\rm tot}(E)}, \tag{9}$$

where $\Gamma^0_{ee} = \Gamma_{ee}/(1+\delta_{\rm vp})$, M and Γ_{ee} are the mass and leptonic width of the $\psi(3770)$ resonance respectively; E is the center-of-mass energy; $\Gamma_{\rm tot}(E)$ is chosen to be energy dependent and normalized to the total width $\Gamma_{\rm tot}$ at the peak of the resonance [7][11]. The $\Gamma_{\rm tot}(E)$ is defined as

$$\Gamma_{\rm tot}(E) = \Gamma_0 \frac{\frac{p^3_{D^0}}{1+(rp_{D^0})^2} + \frac{p^3_{D^\pm}}{1+(rp_{D^\pm})^2}}{\frac{p^{0\,3}_{D^0}}{1+(rp^0{}_{D^0})^2} + \frac{p^{0\,3}_{D^\pm}}{1+(rp^0{}_{D^\pm})^2}}, \tag{10}$$

where p^0_D is the momentum of the D mesons produced at the peak of $\psi(3770)$, p_D is the momentum of the D mesons produced at the c.m. energy $\sqrt{s}$, Γ_0 is the width of the $\psi(3770)$ at the peak, and r is the interaction radius which was set to be 0.5 fm. In the calculation of the Born order cross section, the $\psi(3770)$ resonance parameters $M = 3769.9 \pm 2.5$ MeV; $\Gamma_0 = 23.6 \pm 2.7$ MeV and $\Gamma_{ee} = 0.26 \pm 0.04$ keV [7] were used.

In the structure function approach introduced by Kuraev and Fadin [12][13], the sampling function can be written as

$$f(x,s) \;=\; \beta x^{\beta-1}\delta^{V+S} + \delta^H, \tag{11}$$

where β is the electron equivalent radiator thickness,

$$\beta \;=\; \frac{2\alpha}{\pi}\left(\ln\frac{s}{m_e^2} - 1\right), \tag{12}$$

$$\delta^{V+S} \;=\; 1+\frac{3}{4}\beta+\frac{\alpha}{\pi}\left(\frac{\pi^2}{3}-\frac{1}{2}\right)+\frac{\beta^2}{24}\left(\frac{1}{3}\ln\frac{s}{m_e^2}+2\pi^2-\frac{37}{4}\right), \tag{13}$$

$$\delta^H \;=\; \delta^H_1 + \delta^H_2, \tag{14}$$

$$\delta^H_1 \;=\; -\beta\left(1-\frac{x}{2}\right), \tag{15}$$

$$\delta^H_2 \;=\; \frac{1}{8}\beta^2\left[4(2-x)\ln\frac{1}{x} - \frac{1+3(1-x)^2}{x}\ln(1-x) - 6 + x\right]. \tag{16}$$

In the above formula, m_e is the electron mass and α is the fine structure constant. The $\psi(3770)$ width (~ 24 MeV) is much large than the energy spread (~ 1.37 MeV) of BEPC. So the effect of the beam energy spread on the cross section could be ignored. The $\psi(3770)$ is generally assumed to decay exclusively into $D\bar{D}$. Taking these considerations, the observed cross section of Equation (7) should be replaced by

$$\sigma^{\rm obs}(s) = (1+\delta_{VP})\int_0^{1-4M_D^2/s} dx \cdot f(x,s)\sigma^B(s(1-x)) \tag{17}$$

in calculation of the radiative corrections. The correction factor for the radiative effects is given by

$$g = \frac{\sigma^{\rm obs}}{\sigma^B}. \tag{18}$$

Figure 2 shows the factor of the radiative corrections as a function of the nominal center-of-mass energy. At the center-of-mass energy $\sqrt{s} = 3.773$ GeV, the factor is

$$g = 0.779 \pm 0.031, \tag{19}$$

where the error is the uncertainty arising from the errors on the $\psi(3770)$ resonance parameters. The uncertainty is mainly due to the error of the mass of the resonance.

VII. CROSS SECTION FOR $D\bar{D}$ PRODUCTION

The tree level cross section for $D\bar{D}$ production is obtained by dividing the observed cross section by the factor of the radiative corrections. At $\sqrt{s} = 3.773$ GeV, the charged, neutral and total tree level D pair production cross sections are

$$\sigma_{D^0\bar{D}^0} = (4.60 \pm 0.12 \pm 0.45) \;\; \text{nb}, \tag{20}$$

$$\sigma_{D^+D^-} = (3.29 \pm 0.10 \pm 0.37) \;\; \text{nb}, \tag{21}$$

and

$$\sigma_{D\bar{D}} = (7.88 \pm 0.15 \pm 0.74) \;\; \text{nb}, \tag{22}$$

where the first error is statistical and the second systematic which include the uncertainty in the factor of the radiative corrections. These results are compared to the coupled-channel model prediction in Table V.

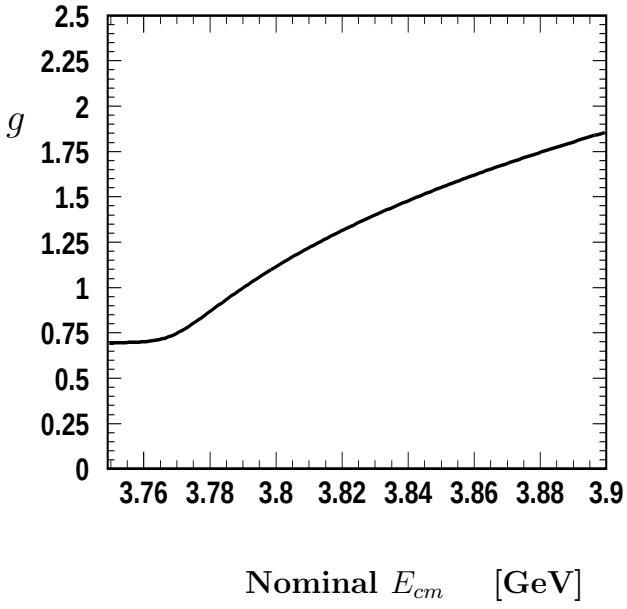

FIG. 2: The factor of radiative corrections as a function of the nominal center-of-mass energy.

TABLE V: Comparison of tree level cross section measurements with prediction of the coupled-channel model at $\sqrt{s} = 3.773$ GeV.

	Experiment	coupled-channel Model
$\sigma_{D^0\bar{D}^0}$	$4.60 \pm 0.12 \pm 0.45$ nb	1.80 nb
$\sigma_{D^+D^-}$	$3.29 \pm 0.10 \pm 0.37$ nb	1.28 nb
$\sigma_{D\bar{D}}$	$7.88 \pm 0.15 \pm 0.74$ nb	3.08 nb

VIII. MEASUREMENT OF R_D AND R

The tree level cross section for $\mu^+\mu^-$ production in QED is given by

$$\sigma_{e^+e^-\to\mu^+\mu^-} = \frac{86.8 \text{ nb}}{E_{cm}^2}, \tag{23}$$

where the E_{cm} is the center-of-mass energy in GeV. A measurement of R_D [4] is obtained by dividing $2\sigma_{D\bar{D}}$ by the tree level muon pair cross section, which gives

$$R_D = 2.58 \pm 0.05 \pm 0.24. \tag{24}$$

BES-II experiment measured R_{uds}[14], which is the ratio of the tree level light hadron (containing the u,d and s light quarks) cross section over that for $\mu^+\mu^-$ production in the energy region from 2.0 to 3.0 GeV. Theoretical expectation is that R_{uds} is approximately independent of center-of-mass energy in this region [3]. Fitting to the R_{uds} values at 9 energy points in the energy region, we obtain $R_{uds} = 2.26 \pm 0.14$. Assuming that $\psi(3770)$ decays exclusively into $D\bar{D}$, the value of R is evaluated using $R = R_D/2 + R_{uds}$, which gives

$$R = 3.55 \pm 0.03 \pm 0.18. \tag{25}$$

IX. SUMMARY

In summary, using the 17.3 pb^{-1} of data collected with the BES-II detector at BEPC at center-of-mass energy $\sqrt{s} = 3.773$ GeV, the observed cross sections for $D^0\bar{D}^0$, D^+D^- and $D\bar{D}$ production have been measured. Those are $\sigma^{\rm obs}_{D^0\bar{D}^0} = (3.58 \pm 0.09 \pm 0.31)$ nb, $\sigma^{\rm obs}_{D^+D^-} = (2.56 \pm 0.08 \pm 0.26)$ nb and $\sigma^{\rm obs}_{D\bar{D}} = (6.14 \pm 0.12 \pm 0.50)$ nb. The tree level cross sections for the $D^0\bar{D}^0$, D^+D^- and $D\bar{D}$ production are determined to be $\sigma_{D^0\bar{D}^0} = (4.60 \pm 0.12 \pm 0.45)$ nb, $\sigma_{D^+D^-} = (3.29 \pm 0.10 \pm 0.37)$ nb and $\sigma_{D\bar{D}} = (7.88 \pm 0.15 \pm 0.74)$ nb, which are about a factor 2.5 times larger than that predicted by the coupled-channel model. Using the measured R_{uds} in the energy region from 2.0 to 3.0 GeV from BES-II experiment and assuming that $\psi(3770)$ only decays to $D\bar{D}$, the total tree level cross section for inclusive hadronic event production at 3.773 GeV is obtained to be $R = 3.55 \pm 0.03 \pm 0.18$.

ACKNOWLEDGEMENTS

The BES collaboration thanks the staff of BEPC for their hard efforts. This work is supported in part by the National Natural Science Foundation of China under contracts Nos. 19991480,10225524,10225525, the Chinese Academy of Sciences under contract No. KJ 95T-03, the 100 Talents Program of CAS under Contract Nos. U-11, U-24, U-25, and the Knowledge Innovation Project of CAS under Contract Nos. U-602, U-34(IHEP); by the National Natural Science Foundation of China under Contract No.10175060(USTC),and No.10225522(Tsinghua University).

[1] E. Eichten *et al.*, Phys. Rev. **D21**, 203 (1980).
[2] J.L. Rosner, hep-ph/0405196 v2.
[3] J.Z. Bai *et al.*, (BES Collaboration), Phys. Rev. **D62**, 012002-1 (2000).
[4] M.W. Coles et al. Phys. Rev. **D26**, 2190 (1982).
[5] J.Z. Bai *et al.* (BES Collaboration), Nucl. Instr. Meth. **A458**, 627 (2001).
[6] BES Collaboration, M. Ablikim *et al.*, Phys. Lett.

B597(2004)39. A Gaussian function was assumed for the signal. The background shape was

$$(1.0 + p_1 y + p_2 y^2) N \sqrt{1 - (\frac{x}{E_b})^2} x e^{-f(1-\frac{x}{E_b})^2},$$

where $N\sqrt{1 - (\frac{x}{E_{\rm beam}})^2} x e^{-f(1-\frac{x}{E_{\rm beam}})^2}$ is ARGUS background shape, x is the fitted mass, $E_{\rm beam}$ is the beam energy, $y = (E_{\rm beam} - x)/(E_{\rm beam} - 1.82)$, N, f, p_1 and p_2 are the fit parameters; The ARGUS background shape was used by ARGUS experiment to parametrize the background for fitting B mass peaks. For detail, see: Ian C. Brock, Mn-Fit, a Fitting and plotting package using MINUIT, Version 4.07, December 22, 2000.

[7] K. Hagiwara *et al.* (Particle Data Group), Phys. Rev. **D66** (2002).

[8] R.H. Schindler *et al.*, Phys. Rev. **D24**, 78(1981).

[9] I. Peruzzi *et al.*, Phys. Rev. Lett. **39**, 1301(1977), D.L. Scharre *et al.*, Phys. Rev. Lett. **40**, 74(1978).

[10] J. Adler *et al.*, Phys. Rev. Lett. **60**, 89(1988).

[11] R.H. Schindler *et al.*, Phys. Rev. **D21** 2716(1980).

[12] E.A. Kuraev and V.S. Fadin, Sov. J. Nucl. Phys. 41(1985)466.

[13] G. Altarelli and G. Martinelli, CERN Yellow Report 86-02(1986)47; O. Nicrosini and L. Trentadue, Phys. Lett. B196(1987)551.

[14] J.Z. Bai *et al.*, (BES Collaboration), Phys. Rev. Lett. **88**, 101802-1 (2002).